

7-26-1990

Advances in Corrosion Casting Methods

K. C. Hodde
Academic Medical Center

D. A. Steeber
University of Wisconsin

R. M. Albrecht
University of Wisconsin

Follow this and additional works at: <https://digitalcommons.usu.edu/microscopy>



Part of the [Life Sciences Commons](#)

Recommended Citation

Hodde, K. C.; Steeber, D. A.; and Albrecht, R. M. (1990) "Advances in Corrosion Casting Methods," *Scanning Microscopy*. Vol. 4 : No. 3 , Article 17.

Available at: <https://digitalcommons.usu.edu/microscopy/vol4/iss3/17>

This Article is brought to you for free and open access by the Western Dairy Center at DigitalCommons@USU. It has been accepted for inclusion in Scanning Microscopy by an authorized administrator of DigitalCommons@USU. For more information, please contact digitalcommons@usu.edu.



ADVANCES IN CORROSION CASTING METHODS

K.C. Hodde¹, D.A. Steeber* and R.M. Albrecht*

Laboratory for Experimental Surgery,
Academic Medical Center,
1105 AZ Amsterdam, The Netherlands.

*Department of Veterinary Science,
University of Wisconsin,
Madison, WI 53706, USA.

(Received for publication June 20, 1990, and in revised form July 26, 1990)

Abstract

This paper briefly discusses the concept of corrosion cast preparation (primarily of blood vessels), the use of the scanning electron microscope (SEM) to study these casts and the observations which can be made, together with the merits and the limitations in various applications. A number of reviews and surveys are quoted in which the different injection media, injection methods, animal preparations and corrosion procedures are described. A new procedure of cleaning the corrosion casts with sodium hydroxide and Triton X-100 is described. The observations which can be made are listed and illustrated both on the cellular level as well as in organ systems as a whole. The discussion centers around some common misconceptions, the feasibility in various applications and the limitations of the method.

The conclusion is that the method has proven to be useful especially in conjunction with other methods. Moreover, while the concept of the method may be very straight-forward the approach and the interpretation often need careful consideration and might not be as straight-forward as one tends to expect from the simple sounding principle.

Key Words: Vascular Corrosion Casting; Scanning Electron Microscopy; Corroding Procedures; Blood Vessels; Lymph Node.

¹Address for correspondence:

K.C. Hodde
Laboratory for Surgical Research
Academic Medical Center
Meibergdreef 9
1105 AZ Amsterdam
The Netherlands
Phone: 31 20 5665571

Introduction

Soon after the scanning electron microscope (SEM) was available commercially, the long existing and extensively used concept of corrosion casting was introduced in the field of scanning electron microscopy. Corrosion casts are produced by filling an internal luminal system or space with a liquid medium which becomes solid *in situ*. The surrounding tissue is then corroded and removed. The resulting replica is then dried, rendered conductive and examined in the SEM. In the first publications synthetic rubber (Nowell *et al.*, 1970) and acrylic resin (Murakami, 1971) were used. Various modifications have led to the now routinely used low viscosity proprietary and non-proprietary rubbers and resins.

A number of surveys have reviewed the literature on corrosion casting. Because the number is still restricted and because each group of authors has specific areas of interest it is advisable to refer to each of these to get an overview. A guiding selection could be: Christofferson and Nilsson, 1988; Hodde and Nowell, 1980; and Lametschwandtner *et al.*, 1984 and 1990. The last two mentioned references contain complete bibliographies.

A number of papers have dealt with the casting materials in particular: Murakami, 1971 (first resin replica); Frasca *et al.*, 1978 (very low viscosity latex); Gannon, 1981 (very low viscosity resin); Hanstede and Gerrits, 1982 (araldite as injection medium); Murakami *et al.*, 1984 (hydrophilic resin), whereas others have established physical properties of the media (Weiger *et al.*, 1986b) and compared results of the various media (Christofferson and Nilsson, 1988).

Some of the above authors and others have dealt with the method as such: Schraufnagel and Schmid, 1988a and 1988b; Christofferson, 1988; Schraufnagel, 1987; Lametschwandtner *et al.*, 1984 and 1990; Castenholz, 1983 (light microscopy of cast *in situ* in fixed tissue); Castenholz *et al.*, 1982 (very complete treatment of leakage artifacts), and Hodde and Nowell, 1980 (the history of the method and discussion of different approaches).

At present there is no generally accepted procedure for the corrosion of the specimens into clean

ones, nor is the literature consistent on this point. Moreover, in perfusion-fixed tissue preparations the corrosion sometimes causes problems and always takes more time. All kinds of corrosive agents (alkaline, acid, with or without detergents and/or sonication or other mechanical means) have been and still are being used. We systematically looked at an alkaline corrosive agent in combination with Triton X-100.

Materials and Methods

Animals

For these studies inbred Balb/c mice between the ages of eight and twelve weeks were used.

Corrosion Casting

Mice were anesthetized with a subcutaneous injection of 0.15 ml ketamine hydrochloride (100 mg/ml) containing Rompun (0.25 mg/ml). The thoracic cavity was opened and 0.05 ml heparin (1000 U/ml) was injected into the left ventricle and allowed to circulate. The left ventricle was punctured and a polyethylene cannula (Intramedic PE 100) was inserted into the aorta and held in place with a silk thread tied around the aorta. The right atrium was opened to serve as an efferent port. The animals were then perfused manually with 20 ml of a modified Krebs buffer, pH 7.4, containing calcium (1.5 mM), dextrose (0.17%), heparin (10 U/ml), sodium nitrite (3 mM) and BSA (1%) warmed to 37°C. For unfixed samples, mice were further perfused with 0.1 M phosphate buffer (pH 7.4) using a Harvard infusion/withdrawal pump (South Natick, MA) at a rate of 5 ml/min for 15 minutes. When fixed samples were desired the 0.1 M phosphate buffer was supplemented with glutaraldehyde (0.5% final concentration) and the animals perfused as above. Following perfusion, all animals were cast by manually injecting 10 ml of a 1:1 mixture of Mercor CL-2B® to methylmethacrylate monomer (final viscosity of 3-4 cps) containing 0.16 g catalyst/ml of mixture (all from Ladd, Burlington, VT). Polymerization was completed by incubating the animals in a 50°C water bath for 2 hours. The desired tissues were dissected out for subsequent corrosion.

Corrosion

The various corrosion treatments used on the cast tissues (either whole or dissected pieces) were as follows:

Sodium hydroxide. Pieces of unfixed liver were placed in solutions of 5, 6, 7, 7.5, 8, 9, 10, and 40% sodium hydroxide and were compared for their efficiency of tissue corrosion. Tissues were corroded in petri dishes in an incubator at 45°C. All samples were placed into fresh sodium hydroxide solutions at 12 hour intervals. The samples were evaluated at 24 hour intervals using a dissecting microscope. At this time each sample was awarded a number from 0-4, representing the degree of clearing or digestion that had occurred (a value of 4 was awarded to a cast that appeared to be 100% cleared of tissue). Light

micrographs were also taken at this time.

Sodium hydroxide with Triton X-100. Unfixed whole kidneys were placed in 7.5% sodium hydroxide solution containing either 5% or 20% Triton X-100 (v/v; Sigma, St. Louis, MO). The samples were corroded in petri dishes at 45°C. The samples were placed into fresh solutions at 12 hour intervals, and graded and photographed at 24 hour intervals as described above.

Fixed versus unfixed tissue. Pieces of fixed and unfixed lungs were corroded in 7.5% sodium hydroxide for 24 hours then placed into 5% Triton X-100 for 24 hours. All incubations were carried out at 45°C. The samples were placed into fresh solutions at 12 hour intervals, and graded and photographed at 24 hour intervals as described above.

SEM Preparation

After corrosion the casts were thoroughly rinsed in several changes of distilled water, dissected (if necessary) and air dried from 100% sieve-dried ethanol. In some cases the casts were first further cleaned by placing them into an 80 W sonicator for 15 minutes (Heat System Ultrasonics Inc., Plainview, NY). All casts were then mounted with epoxy on stubs, grounded with silver paint, sputter coated with 20 nm gold-palladium and viewed with a Hitachi model S-570 scanning electron microscope at 5-10 kV accelerating voltage.

Results

The concentration of sodium hydroxide used in the clearing process was found to have an effect upon the efficiency of corrosion. The 40% solution showed minimal tissue corrosion even after nine days, perhaps due to protein cross-linking and lipid saponification. This was especially true of tissues which contained or were surrounded by large amounts of fat (e.g. lymph nodes within fatpad). All concentrations of sodium hydroxide in the range of 5-10% appeared

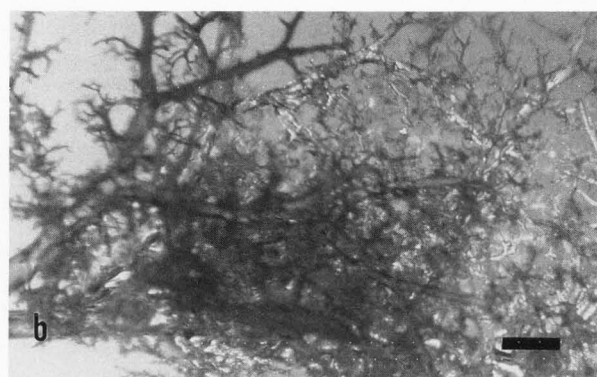
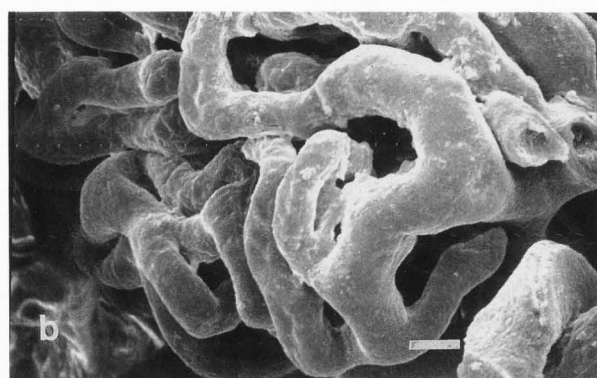
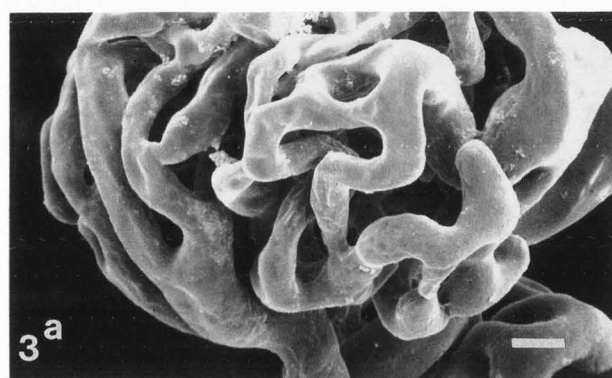
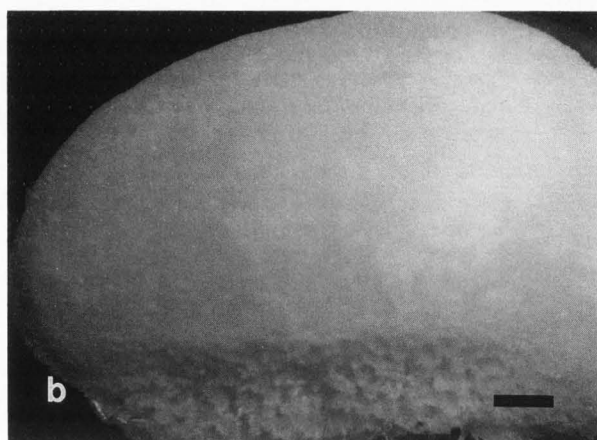
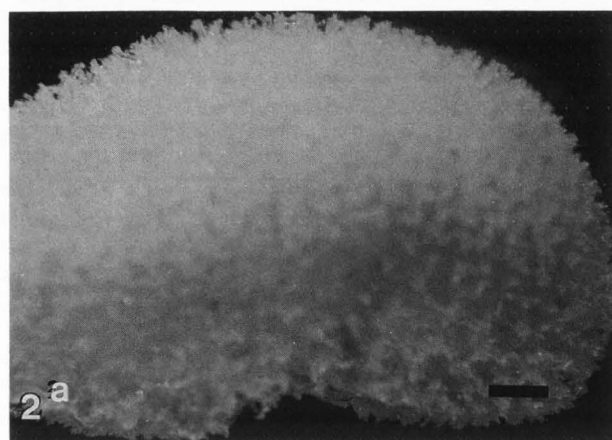
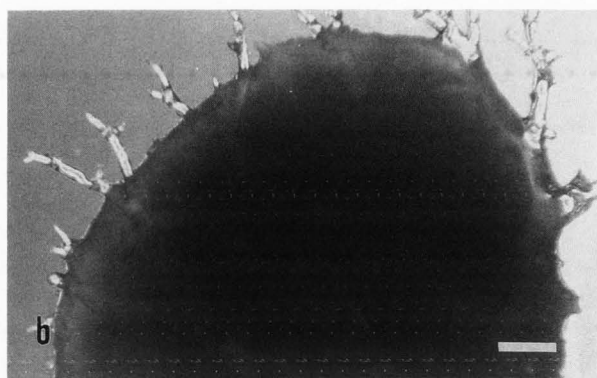
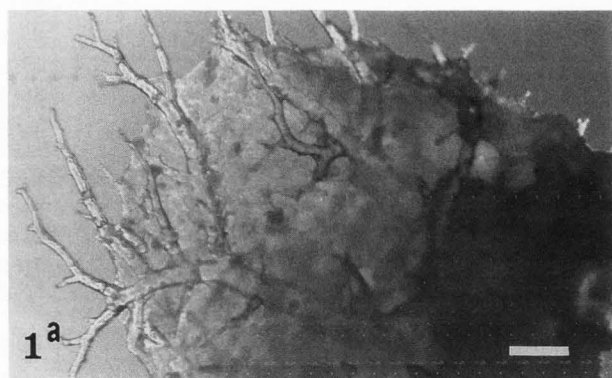
Figure 1: Light micrographs of cast unfixed liver tissue after 4 days corrosion in (a) 7.5% and (b) 40% sodium hydroxide at 45°C. Bars = 1 mm.

Figure 2: Light micrographs of cast unfixed whole kidneys following 9 days in 7.5% sodium hydroxide at 45°C supplemented with (a) 5% and (b) 20% Triton X-100. Bars = 1 mm.

Figure 3: (a) Scanning electron micrograph of a glomerulus from the sample illustrated in figure 2a and dried on day 9; (b) idem, glomerulus from figure 2b. Bars = 5 µm.

Figure 4: Light micrographs of cast lung tissue corroded for 24 hours in 7.5% sodium hydroxide followed by 24 hours in 5% Triton X-100 (a) unfixed and (b) fixed lung. Bars = 1 mm.

Advances in Corrosion Casting Methods



relatively equally effective, although sodium hydroxide alone at any concentration was not as effective in corroding the tissue as when used in conjunction with detergent. Figure 1 shows the increased digestion of liver tissue that occurs in 7.5% sodium hydroxide (Fig. 1a) as compared to 40% sodium hydroxide (Fig. 1b) after 4 days of corrosion.

Both alternate 24 hour washes in 7.5% sodium hydroxide followed by Triton X-100 and the direct addition of Triton X-100 detergent to the sodium hydroxide (even though the Triton X-100 was not completely soluble in the sodium hydroxide) were effective in reducing the time to clear the casts of tissue. The 5% Triton X-100 solution was found to be equally effective as the 20% solution. Total clearing of the casts was often achieved within 48 hours. Sonication did not appear to damage the casts and was effective in cleaning the small amount of residual material which is often present from the casts.

Recently it has been described by Schraufnagel and Schmid (1988b) that light microscopy of wet samples is not the optimal means of assessing the extent of corrosion. Our results further substantiate this claim. The kidney samples shown in figure 2 appear as though the corrosion had progressed differentially when the sodium hydroxide was supplemented with 5% (Fig. 2a) or 20% (Fig. 2b) Triton X-100 after nine days of treatment. When the same samples are observed by scanning electron microscopy after drying they are both seen to be completely cleared of tissue (Figs. 3a, 3b respectively). We attribute the apparent difference noted by light microscopy to be due to a difference in the number of vessels per unit area (i.e. vessel density) in the casts.

We were unable to detect any difference in the corrosion time of fixed versus unfixed tissue. Figure 4 illustrates lung tissue that had been cast without prior fixation (Fig. 4a), or fixed by perfusion with 0.5% glutaraldehyde prior to casting (Fig. 4b). After corrosion in 7.5% sodium hydroxide for 24 hours, followed by treatment with 5% Triton X-100 for 24 hours, the casts of both fixed and unfixed tissues are observed to be completely cleared of tissue. We noted similar results with all tissues examined.

Typical tissue remnants are observed surrounding a cast vessel following incomplete corrosion (Fig. 5). This pattern is distinctly different from that of resin leakage as shown in figure 6. In this case typical ring-shaped profiles surrounding the cast vessel are seen (see Castenholz *et al.*, 1982 for an extensive discussion on the subject). Veins and arteries show different and consistently recognizable imprint patterns from the endothelial lining (Miodonski *et al.*, 1976; Hodde *et al.*, 1977) (Figs. 7-10). These patterns can be distinguished from other features such as trapped and/or attached blood cells (Fig. 11). The typical round versus oval endothelial cell nuclei imprints and the polygonal versus oval endothelial cell border imprints retain their shapes even in a contracted or distended condition (Figs. 9, 10 respec-

tively).

The endothelial cell cushion configuration described previously by many authors (Wagenvoort, 1954; Fourman and Moffat, 1961) show up very clearly in cast preparations of arterial branching sites as demonstrated in figure 12. These have also been described by Hodde, 1981a; Casellas *et al.*, 1982; Kardon *et al.*, 1982 and Murata *et al.*, 1982. Fourman and Moffat (1961) concluded from *in vivo* observations that the cushion profile protruding into the lumen samples the cell-rich axial stream, thus producing "cell-skimming."

Arteriovenous anastomosis, when filled with this method, can be established beyond any doubt. Figures 13 and 14 show an example in the nasal circulation of the rat. The direct arteriovenous connections are visible (Fig. 13) with diameters exceeding those of capillaries at least five-fold. Endothelial cell imprint patterns of arteriovenous anastomoses display an intermediate appearance from that of arteries and veins (Fig. 14).

Another pattern that is typically found in the lymph node vasculature is that of the high endothelial venules (Figs. 15, 16). These venules can be identified in the cast by the characteristic pattern of deep impressions which match the dimensions of the endothelial cells (Steeber *et al.*, 1987; Castenholz, 1990).

Retrogradely filled veins show the shut venous valve contours as shown in figure 17. This feature has

Figure 5: SEM of cast blood vessel surrounded by incompletely digested tissue remnants. Bar = 10 μ m.

Figure 6: Idem, surrounded by plastic rings resulting from leakage of the injection medium through the vessel wall (reprinted from Hodde and Nowell, 1980). Bar = 20 μ m.

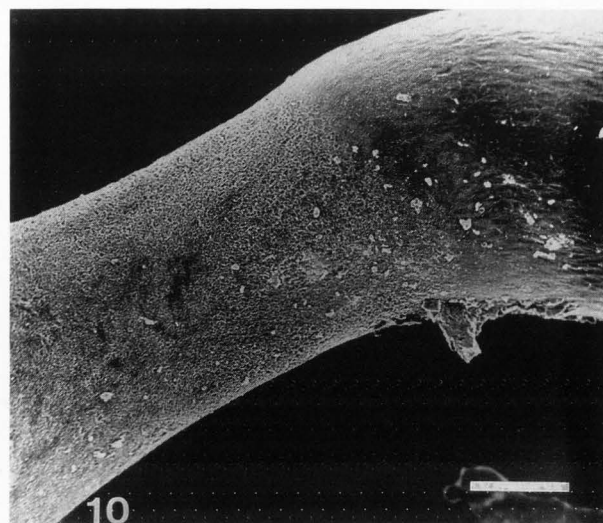
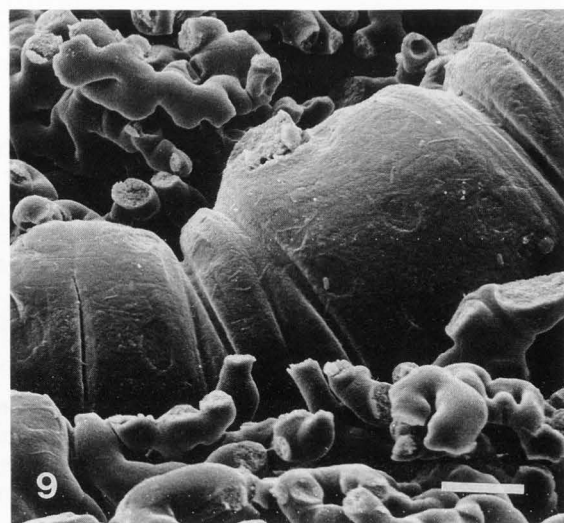
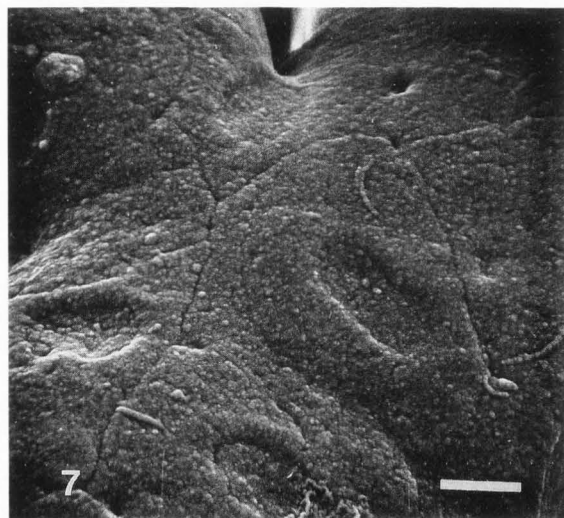
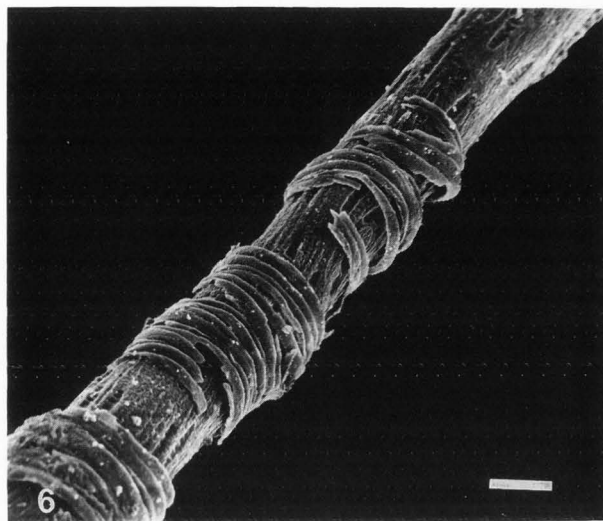
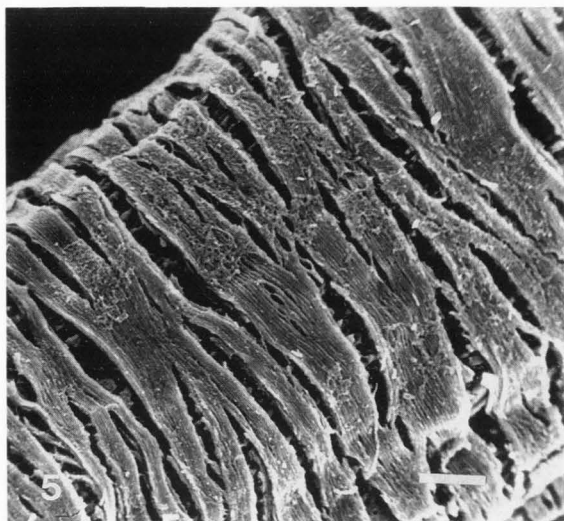
Figure 7: Cast of a vein. Round imprints of endothelial cell nuclei (foreshortened in perspective) and cell border imprints forming polygonal patterns are seen. Bar = 10 μ m.

Figure 8: Cast of an artery. Endothelial cell nuclei imprinted as oval shapes oriented in the length axis of the vessel. Cell borders form similar patterns which are seen as grooves surrounding the nuclei in a parallel fashion. Bar = 10 μ m.

Figure 9: Cast of a constricted vein in lung parenchyma with band-shaped constrictions. Nuclear imprints are still recognizable beyond doubt as venous. Bar = 20 μ m.

Figure 10: Cast of a rat stapedial artery. Left half: part of vessel cast previously running through Stapes. Right part: free, distended part. Endothelial cell nuclear imprints and cell border imprints are still oval in shape. Bar = 100 μ m.

Advances in Corrosion Casting Methods



been used to check the (in-) competence of experimentally damaged valves (Van Bemmelen *et al.*, 1986)(Fig. 18).

For some studies it is necessary to keep skeletal parts intact as a reference to the spacial distribution of the blood vessels. In figure 19 this was obtained by enzymatic digestion in a detergent for one week at 37°C. The viscosity of the resin injected was such that only the arterial part (Fig. 20) or the venous part was filled and thus further dissection was not necessary.

The complete blood vasculature of a whole organ or part thereof can be demonstrated with this method of corrosion casting (Figs. 21-28) either with little dissection, e.g. incisor teeth (Hodde *et al.*, 1983) (Figs. 21, 22) and pineal gland (Figs. 23 and 24) or with much time-consuming preparatory dissection, e.g. rat hypophysis (Figs. 25, 26) and the rat choroid plexus of the lateral ventricle (Hodde, 1979b; Weiger *et al.*, 1986a) (Figs. 27, 28).

Discussion

As is obvious from the extensive bibliography (Lametschwandtner *et al.*, 1984 and 1990) the corrosion casting method used with SEM has been applied in various areas to address questions of "functional anatomy" in developmental anatomy (Caduff *et al.*, 1986), hormone transport in the Pineal gland, (Hodde, 1979a), hypophysis (Bergland and Page, 1978; Hodde, 1981b), nasal circulation and temperature regulation (Hodde, 1986), hypertension (Hodde *et al.*, 1984), immunology (Steeber *et al.*, 1987), pathophysiology of venous valves (Van Bemmelen *et al.*, 1986), pharmacology (Olson, 1980), vasoproliferation (Burger *et al.*, 1984; Christofferson, 1988) and neovascularization (Grunt *et al.*, 1986; Walmsley *et al.*, 1987; Christofferson, 1988). Closed systems have also been studied with this method such as milk ducts (Shenkman *et al.*, 1985) and bile canaliculi (Yamamoto and Phillips, 1984; Gaudio *et al.*, 1988; Schellens *et al.*, 1988).

Questions concerning the degree to which the vascular corrosion casts reflect the *in vivo* situation, before the injection of medium, have been raised because vasomotor activity has been demonstrated to occur with this method (Olson, 1980; Motti *et al.*, 1987). These questions are difficult to answer at this time because many factors may play a role such as the injection pressure and the subsequent intraluminal pressure, the viscosity, the shear stress of the medium with the wall of the vessel, and the direct vasoactive influence of the medium upon the vessel wall. Prefixation of the blood vessels might preclude a number of these factors but has some unknowns of its own in terms of vasomotor reaction to the fixative (Beringer, 1979; Smith and Reese, 1980; Bachofen *et al.*, 1982; Walter *et al.*, 1983; Wisse *et al.*, 1984).

One merit of the corrosion casting method is the fact that the cast shows the real 3-D spatial

measurements since the injection medium becomes solid *in situ*. Although most media shrink measurably (Weiger *et al.*, 1986b) this does not cause volume shrinkage of the preparation *in toto*. This has to be kept in mind when comparing the results with measurements from fixed and processed (dehydrated, CPD etcetera) tissue with 50% shrinkage or more (Boyde and Maconnachie, 1979).

Sometimes the study of vascular cast preparations gives much information with a small effort in time and energy; mostly however, this is not the case and patience becomes another important resource.

References

- Bachofen H, Ammann A, Wangenstein D, Weibel ER. (1982). Perfusion fixation of lungs for structure-function analysis: credits and limitations. *J Appl Physiol* 53: 528-533.
- Bergland RM, Page RB. (1978). Can the pituitary secrete directly to the brain? (Affirmative anatomical evidence). *Endocrinol* 102: 1325-1338.
- Beringer T. (1979). Stereologic analysis of relative blood flow rates from kidney sections. *Anat Rec* 193: 482A.
- Boyde A, Maconnachie E. (1979). Volume changes during preparation of mouse embryonic tissue for SEM. *Scanning Electron Microsc.* 1979; II: 149-163.

Figure 11: Cast of a vein in the rat nasal mucosa. Trapped and/or attached blood cell imprints recognized as such. Bar = 10 µm.

Figure 12: Cast of a branched artery, flow direction was from right to left. Arterial endothelial nuclear and cell border imprints are seen. At branching sites imprints or arterial endothelial cell cushions are seen as grooves deepening into the lumen of the parent vessel towards the left. Bar = 50 µm.

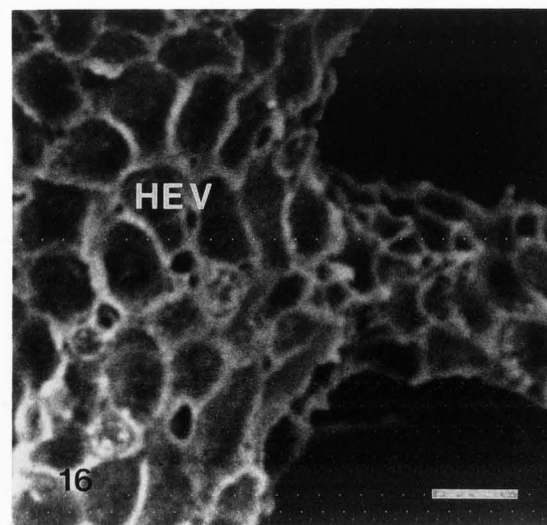
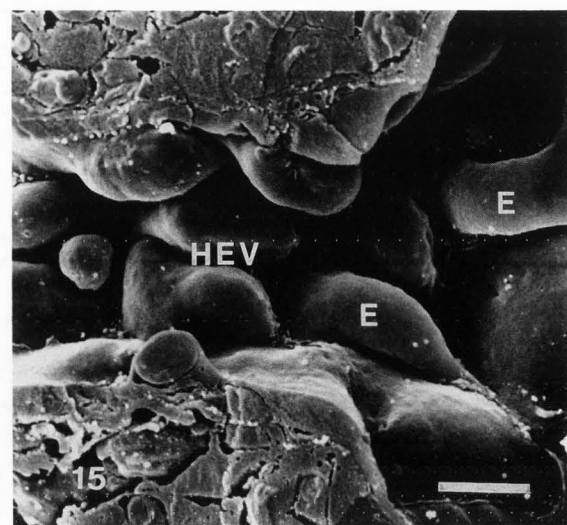
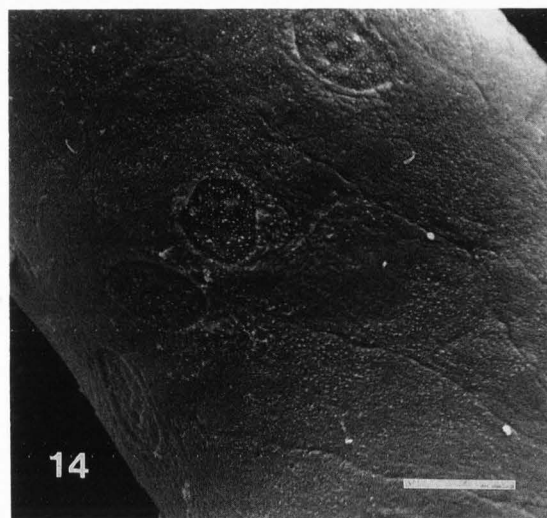
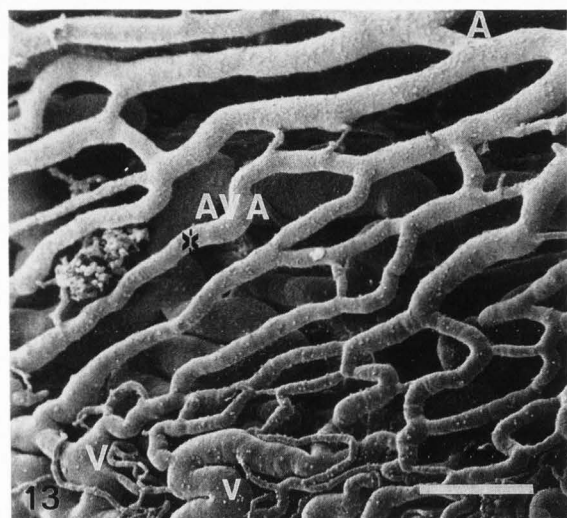
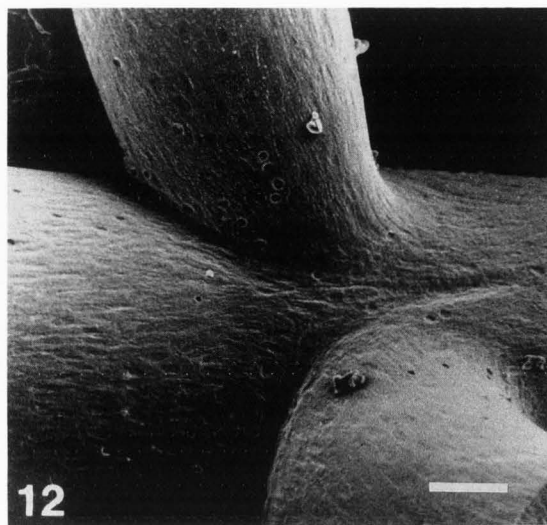
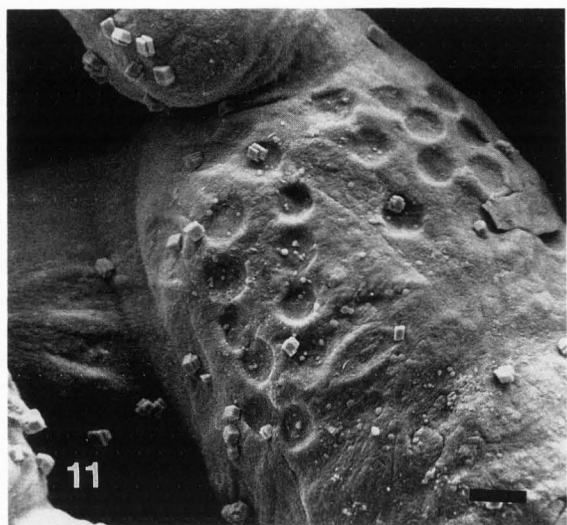
Figure 13: Cast of rat nasal septum vessels. Top: arteries (A). Bottom: veins (V). Middle: arteriovenous anastomoses (AVA). Bar = 50 µm.

Figure 14: Detail of previous figure, note the shape of the endothelial cell nuclear imprints are round and elongated cell border imprints are seen. Bar = 10 µm.

Figure 15: Scanning electron micrograph of a freeze-fractured mouse lymph node showing the lumen of a high endothelial venule (HEV). The prominent endothelial cells (E) are clearly seen. Bar = 5 µm.

Figure 16: Corrosion cast of a high endothelial venule (HEV). The large bulging cuboidal endothelial cells, as shown in figure 15, produce a characteristic and consistently recognizable pattern which can be used to identify the vessel as a HEV. Bar = 10 µm.

Advances in Corrosion Casting Methods



Burger PC, Chandler DB, Drysdale DB, Tano Y, Crapo JD, Freeman BA, Klintworth GK. (1984). SEM of vascular casts in experimental ocular vasoproliferation. *Scanning Electron Microsc.* 1984; IV: 1893-1898.

Caduff JH, Fischer LC, Burri PH. (1986). SEM study of the developing microvasculature in the postnatal rat lung. *Anat Rec* 216: 154-164.

Casellas D, Dupont M, Jover B, Mimran A. (1982). SEM study of arterial cushions in rats: a novel application of the corrosion-replication technique. *Anat Rec* 203: 419-428.

Castenholz A. (1983). The outer surface morphology of blood vessels as revealed in SEM in resin cast, non-corroded tissue specimens. *Scanning Electron Microsc.* 1983; IV: 1955-1962.

Castenholz A. (1990). Interpretation of structural patterns appearing on corrosion casts of small blood and initial lymphatic vessels. *Scanning Microsc* 3: 315-325.

Castenholz A, Zöltzer H, Erhardt H. (1982). Structures imitating myocytes and pericytes in corrosion casts of terminal blood vessels. A methodical approach to the phenomenon of "plastic strips" in SEM. *Mikroskopie (Wien)* 39: 95-106.

Christofferson RH. (1988). Angiogenesis as induced by trophoblast and cancer cells. Thesis, Uppsala University, 81 pp.

Christofferson RH, Nilsson BO. (1988). Microvascular corrosion casting with analysis in the SEM. *Scanning* 10: 43-63.

Fourman J, Moffat DB. (1961). The effect of intra-arterial cushions on plasma skimming in small arteries. *J Physiol* 158: 374-380.

Frasca JM, Carter HW, Schaffer WA. (1978). An improved latex injection media for replicating the pulmonary microvasculature. *Scanning Electron Microsc.* 1978; II: 485-489.

Gannon BJ. (1981). Preparation of microvascular corrosion casting media: procedure for partial polymerization of methylmethacrylate using ultraviolet light. *Biomed Res* 2 (Suppl.): 227-233.

Gaudio E, Pannarale L, Carpino F, Marinozzi G. (1988). Microcorrosion casting in normal and pathological biliary tree morphology. *Scanning Microsc* 2: 471-475.

Grunt TW, Lametschwandner A, Karrer K, Staindl O. (1986). The angioarchitecture of the Lewis lung carcinoma in laboratory mice. *Scanning Electron Microsc.* 1986; II: 557-573.

Hanstede JG, Gerrits PO. (1982). A new plastic for morphometric investigation of blood vessels, especially in large organs such as the human liver. *Anat Rec* 203: 307-315.

Hodde KC. (1979a). The vascularization of the rat pineal organ. *Progr Brain Res* 52: 39-44.

Hodde KC. (1979b). The vascularization of the choroid plexus of the lateral ventricle of the rat. *BEDO* 12: 395-400.

Hodde KC. (1981a). Cephalic vascular patterns in the rat. Thesis, University of Amsterdam. Rodopi, Amsterdam: 36-38.

Hodde KC. (1981b). Vascular casts of the rat pituitary gland. *BEDO* 14: 593-602.

Hodde KC. (1986). The rat brain vessels-SEM of corrosion casts. In: *Neural regulation of brain circulation*, (Owman C, Hardebo JE eds.), Elsevier Sci Publ, pp. 433-450.

Hodde KC, Boyde A, Reid SA, Reith EJ, Schmid MJ. (1983). The vascular architecture of the rat incisor enamel organ. *BEDO* 16: 431-442.

Hodde KC, Miodonski A, Bakker C, Veltman WA. (1977). SEM of microcorrosion casts with special attention on arterio-venous differences and application to the rat's cochlea. *Scanning Electron Microsc.* 1977; II: 477-484.

Hodde KC, Nordborg C, Johansson BB. (1984). Pial artery casts of normotensive and hypertensive rats. *BEDO* 17: 209-214.

Hodde KC, Nowell JA. (1980). SEM of microcorrosion casts. *Scanning Electron Microsc.* 1980; II: 88-106.

Figure 17: Cast of a retrogradely filled vein showing the profile of a shut bicuspid valve with recognizable blood vessel luminal surface imprinted on the surface of the cast. Bar = 50 μ m.

Figure 18: Cast of a retrogradely filled vein with an experimentally caused incompetent bicuspid valve profile on the right side (compare to figure 17). Bar = 10 μ m.

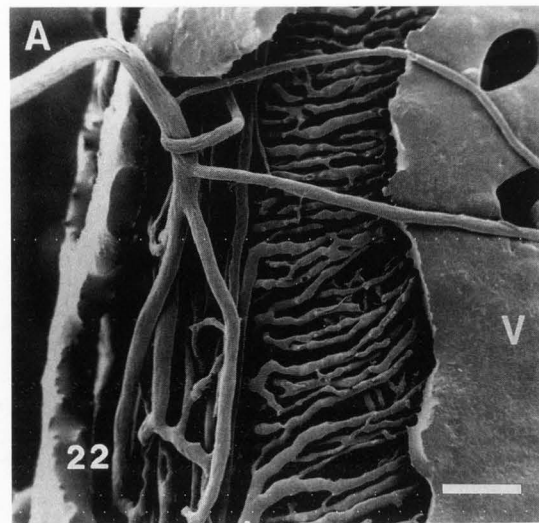
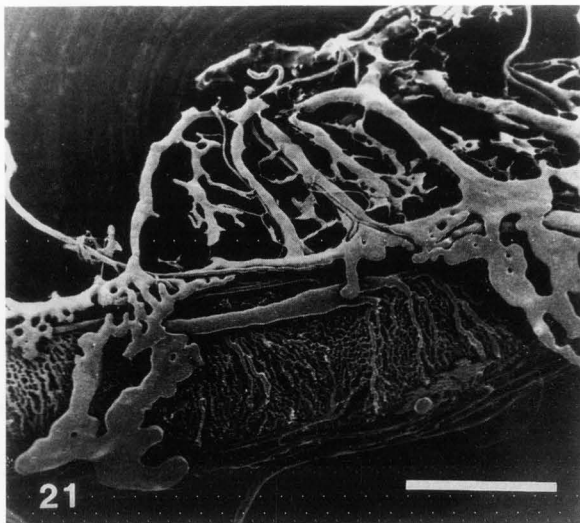
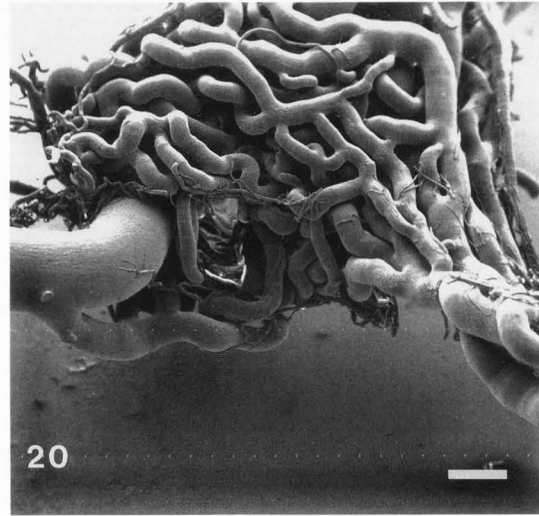
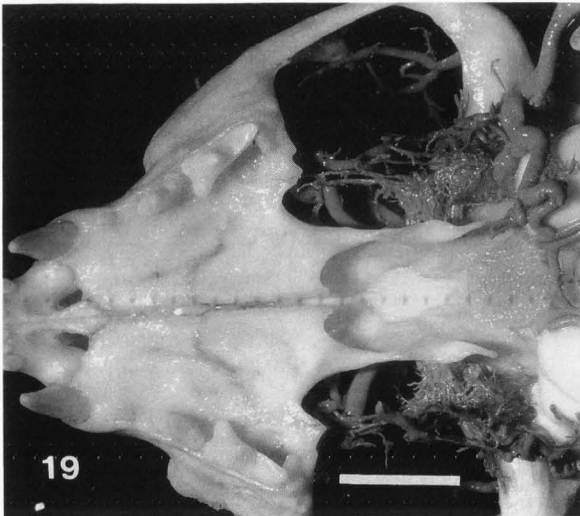
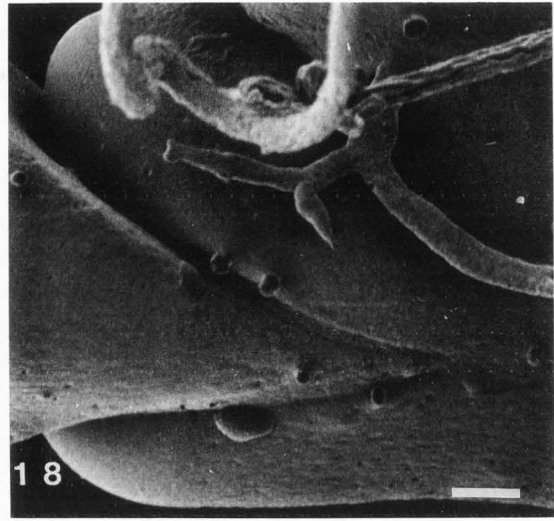
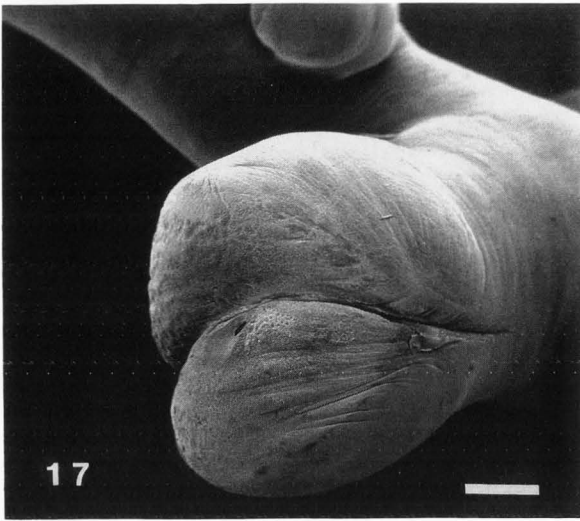
Figure 19: Light micrograph of a cat skull (ventral aspect), with the arterial part of the carotid rete only, injected with high viscosity resin. Tissue corroded completely but the inorganic component of the bone remaining intact. Bar = 10 mm.

Figure 20: Cast of the arterial part of a cat carotid rete. Left: maxillary artery (branch of external carotid). Right: rete vessels joining the internal carotid artery. Bar = 500 μ m.

Figure 21: Rat mandibular incisor tooth. Cast of the complete vascular bed of the enamel organ (ventro-lateral aspect). Incisor end to the left. Bar = 1 mm.

Figure 22: Detail of previous figure (ventral aspect). Supplying arteriole (A) with particular branching pattern feeding into the capillary network of the enamel organ. Indicator A situated at the site of arterial passage through the mandibular foramen. The (V) indicates part of the extensive overlying venous plexus. Bar = 100 μ m.

Advances in Corrosion Casting Methods



Kardon RH, Farley DB, Heidger PM Jr, van Orden DE. (1982). Intra-arterial cushions of the rat uterine artery: a SEM evaluation utilizing vascular casts. *Anat Rec* 203: 19-29.

Lametschwandtner A, Lametschwandtner U, Weiger T. (1984). SEM of vascular corrosion casts - technique and applications. *Scanning Electron Microsc.* 1984; II: 663-695.

Lametschwandtner A, Lametschwandtner U, Weiger T. (1990). SEM of vascular corrosion casts: Technique and applications: Updated review. *Scanning Microsc* 4: (In press).

Miodonski A, Hodde KC, Bakker C. (1976). Rasterelektronenmikroskopie von Plastik-Korrosions-Preparaten: morphologische Unterschiede zwischen Arterien und Venen (SEM of plastic-corrosion casted-samples: morphological differences between arteries and veins). *BEDO* 9: 435-442.

Motti DF, Imhof H-G, Martinez Garza J, Yasargil GM. (1987). Vasospastic phenomena on the luminal replica of rat brain vessels. *Scanning Microsc.* 1: 207-222.

Murakami T. (1971). Application of the SEM to the study of the fine distribution of the blood vessels. *Arch Histol Jap* 32: 445-454.

Murakami T, Itoshima T, Hitomi K, Ohtsuka A, Jones AL. (1984). A monomeric methyl and hydroxypropyl methacrylate injection medium and its utility in casting blood capillaries and liver bile canaliculi for SEM. *Arch Histol Jap* 47: 223-237.

Murata M, Kohchi K, Yoshimoto H. (1982). Valve structure at the arteriolar side arm branching. *J Jap Coll Angiol* 22: 91-101.

Nowell JA, Pangborn J, Tyler WS. (1970). SEM of the avian lung. *Scanning Electron Microsc.* 1970: 249-256.

Olson KR. (1980). Application of corrosion casting procedures in identification of perfusion distribution in a complex microvasculature. *Scanning Electron Microsc.* 1980; III: 357-364.

Schraufnagel DE. (1987). Microvascular corrosion casting of the lung. A state of the art review. *Scanning Microsc* 1: 1733-1747.

Schraufnagel DE, Schmid A. (1988a). Microvascular casting of the lung: vascular lavage. *Scanning Microsc* 2: 1017-1020.

Schraufnagel DE, Schmid A. (1988b). Microvascular casting of the lung: effects of various fixation protocols. *J Elec Microsc Techniques* 8: 185-191.

Schellens JPM, de Haan JG, Hodde KC. (1988). Preparation of injection replicas for SEM studies of the rat biliary system. In: *Inst Phys Conf Ser* 93 vol 3, IOP Publishing, pp. 349-350.

Shenkman DI, Berman DT, Albrecht RM. (1985). Use of polymer casts or metal particle infusion of ducts to study antigen uptake in the Guinea Pig mammary gland. *Scanning Electron Microsc.* 1985; III: 1209-1214.

Smith JE, Reese TS. (1980). Use of aldehyde fixatives to determine the rate of synaptic transmitter release. *J Exp Biol* 89: 19-29.

Steeber DA, Erickson CM, Hodde KC, Albrecht RM. (1987). Vascular changes in popliteal lymph nodes due to antigen challenge in normal and lethally irradiated mice. *Scanning Microsc* 1: 831-839.

Van Bemmelen SP, Hoyneck van Papendrecht AA, Hodde KC, Klopper PJ. (1986). A study of valve incompetence that developed in an experimental model of venous hypertension. *Arch Surg* 121: 1048-1052.

Wagenvoort CA. (1954). Die Bedeutung der Arterien wülste für den Blutkreislauf (The meaning of arterial walls for blood circulation). *Acta Anat* 21: 70-99.

Walmsley JG, Granter SR, Hacker MP, Moore AL, Ershler WB. (1987). Tumor vasculature in young and old hosts: Scanning electron microscopy of microcorrosion casts with microangiography, light microscopy and transmission electron microscopy. *Scanning Microsc* 1: 823-830.

Figure 23: Cast of the rat pineal gland vascular bed which has been dissected free from the surrounding brain vessel cast (lateral aspect). Note the prominently visible draining veins, connected with the left lateral vein (V), which in turn connects with the Confluens Sinuum (CS). Bar = 500 μ m.

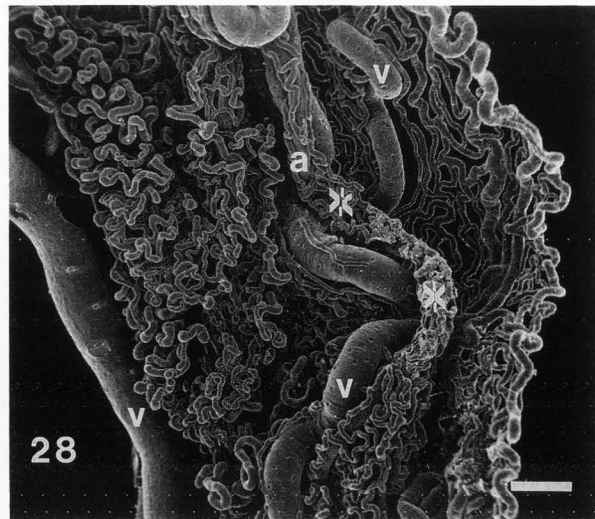
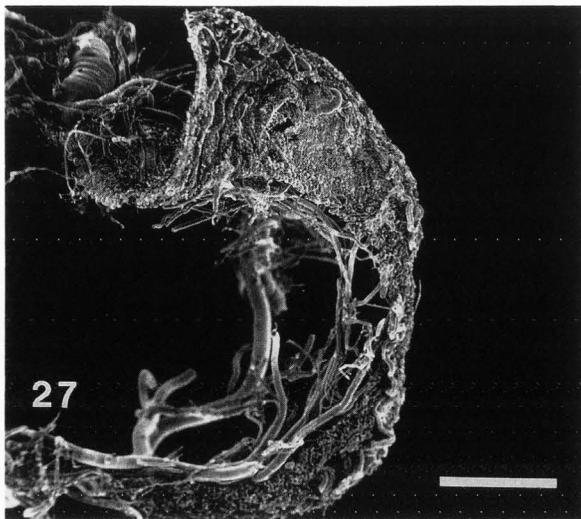
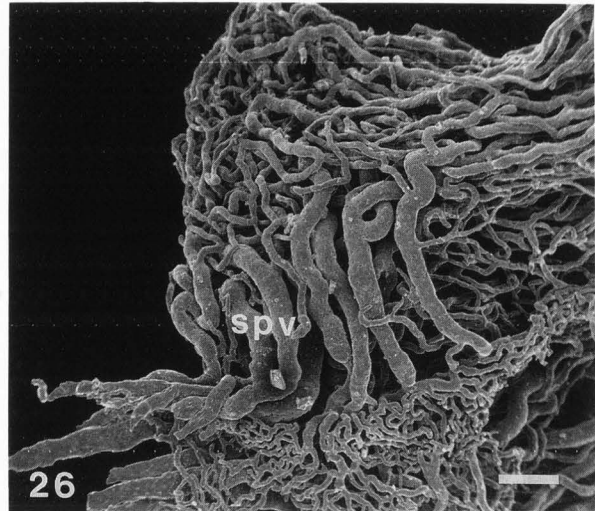
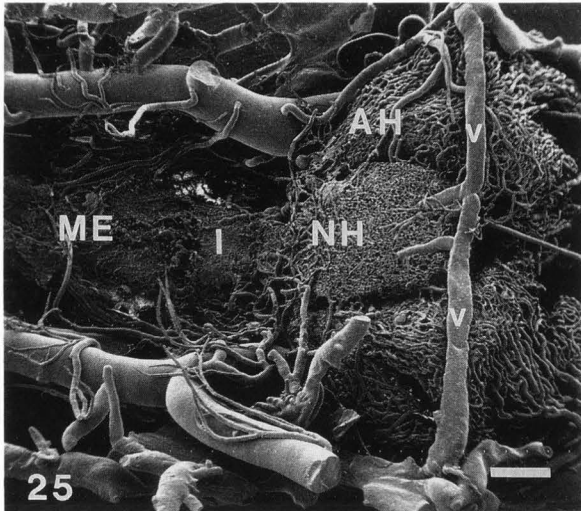
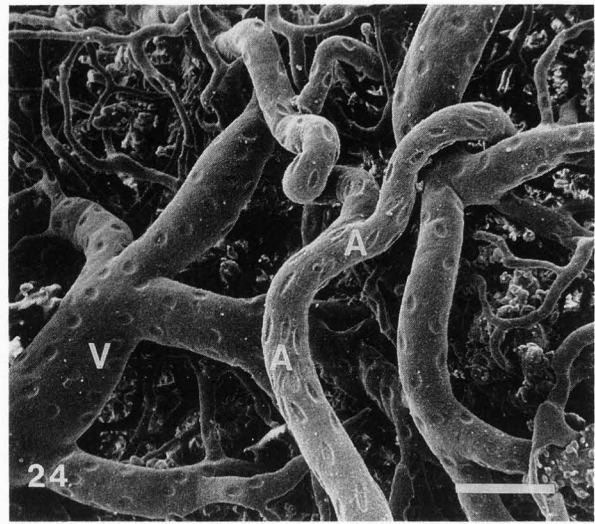
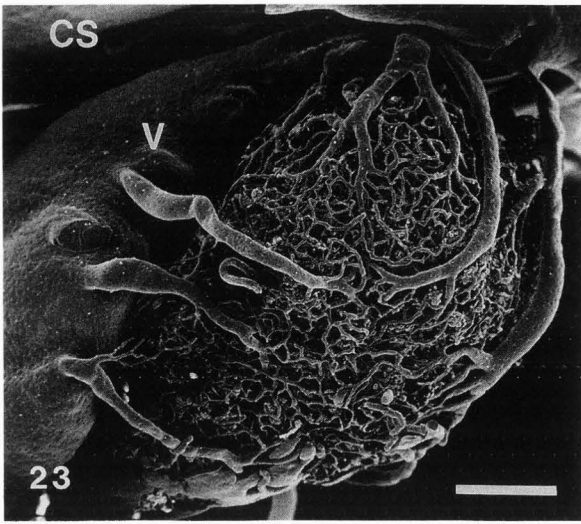
Figure 24: Detail of the previous figure showing supplying arteriole (A) and draining venule (V) at the surface of the pineal gland blood vessel cast. Bar = 100 μ m.

Figure 25: Cast of rat hypophyseal blood vasculature seen from dorsal. Median Eminence (ME), Infundibulum (I), Neurohypophysis (NH), Adenohypophysis (AH), and veins (v) draining the neurohypophysis exclusively. Bar = 500 μ m.

Figure 26: Detail of previous figure. Short portal veins (spv) connecting the neurohypophyseal capillary bed (bottom) with the adenohypophyseal sinusoids (top). Bar = 100 μ m.

Figure 27: Cast of the rat choroid plexus, left lateral ventricle. Seen in fronto-dorsal direction. Bar = 1 mm.

Figure 28: Detail of previous figure. Various capillary patterns shown: forming a flat bed in the free margin (right half picture); in villous formation (left half); and garland type (+) surrounding an artery (a). Veins are prominently seen (v). In the rat, these are never accompanied by the capillaries except for incidental drainage as seen in the center of the picture. Bar = 10 μ m.



Walter GF, Auer LM, Sayama I. (1983). Morphological analysis of contractile elements in pial and intraparenchymal veins after *in vivo* perfusion fixation. In: The cerebral veins, (Auer LM, Loew F eds.), Springer Publ, pp. 57-63.

Weiger T, Lametschwandtner A, Hodde KC, Adam H. (1986a). The angioarchitecture of the choroid plexus of the lateral ventricle of the rabbit. *Brain Res* 378: 285-296.

Weiger T, Lametschwandtner A, Stockmayer P. (1986b). Technical parameters of plastics (Mercox CL-2B and various methylmethacrylates) used in SEM of vascular corrosion casts. *Scanning Electron Microsc.* 1986; 1: 243-252.

Wisse E, De Wilde A, De Zanger R. (1984). Perfusion fixation of human and rat liver tissue for light and electron microscopy: a review and assessment of existing methods with special emphasis on sinusoidal cells and microcirculation. In: Science of biological specimen preparation, (Revel JP, Barnard T, Haggis GH eds.), SEM Inc. AMF O'Hare, IL, pp 31-38.

Yamamoto K, Phillips MJ. (1984). A hitherto unrecognized bile ductular plexus in normal rat liver. *Hepatology* 4: 381-385.

Editor's Note: All of the reviewer's concerns were appropriately addressed by text changes, hence there is no Discussion with Reviewers.